

The “DLR Crash Report”: Towards a Standard Crash-Testing Protocol for Robot Safety - Part II: Discussions

Sami Haddadin, Alin Albu-Schäffer, Mirko Frommberger, Jürgen Rossmann, and Gerd Hirzinger

Abstract—After giving a rich data basis of our impact tests with standardized crash-test dummies in *Part I* of this work we address in *Part II* various aspects related to these tests in a case based discussion. The presented facts, the knowledge gained from our previous work, and the data from *Part I* lead us to recommendations for standardized crash-testing procedures in robotics. The proposed impact procedures will help to compare blunt robot-human impacts on a common basis. We will discuss additional requirements which will enhance the completeness of testing procedures.

I. INTRODUCTION

In *Part I* of this work we discussed the results of various crash-tests we conducted with standardized crash-testing equipment of the German Automobile Club (ADAC). The results were prepared similarly to crash-testing reports known from the automobile industry. Therefore, *Part I* is very result oriented, while detailed evaluations of interesting aspects related to the experiments shall now be given. In order to keep the discussion clearly structured we introduce case discussions that explicitly focus on particular aspects which are from our point of view worth to be treated more in detail.

Standards and guidelines for the evaluation and comparison of safety in physical-human robot interaction are basically still an open issue and were up to now only addressed in [1] from the standardization body’s side. However, the guidelines given there are very restrictive, therefore heavily limiting the performance of the robot, and are presumably not based on a biomechanical analysis of human tolerance data. Subsequent to our short discussions, we give recommendations for standard blunt impact tests which could be a basis for future standardized safety evaluation in robotics. In this sense we contribute a first proposal for a set of standardized robot-dummy crash-tests.

This paper is organized as follows. In Sec. II six case discussions are given which will thematize particular aspects about robot-human impacts. Sec. III will discuss a proposal for standard blunt impact testing in robotics, and finally Sec. IV gives an outlook and Sec. V conclusions.

II. CASE DISCUSSIONS

In this section various aspects which contribute to a deeper understanding of robot-human impacts will be discussed on

S. Haddadin, A. Albu-Schäffer, Mirko Frommberger, and G. Hirzinger are with Institute of Robotics and Mechatronics, DLR - German Aerospace Center, Wessling, Germany sami.haddadin@dlr.de, alin.albu-schaeffer@dlr.de, gerd.hirzinger@dlr.de

Jürgen Rossmann is with Institute of Man-Machine-Interaction, Rheinisch-Westfälische Technische Hochschule Aachen (RWTH), Aachen, Germany rossmann@mimi.rwth-aachen.de

case basis. Cases 1-4 treat unconstrained head and chest impacts, case 5 partially constrained impacts, and case 6 constrained quasistatic impacts. We believe such detailed discussions are important in order to extract the relevant information to be taken into account for future standards.

A. Case 1: The Saturation of the Head Injury Criterion

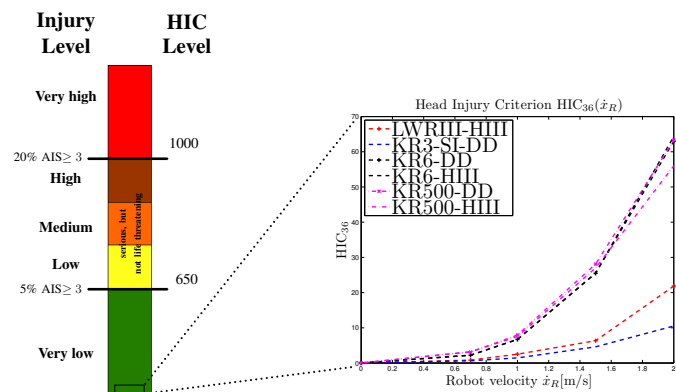


Fig. 1. Resulting HIC_{36} values at varying impact velocities for robots of different weights: the 15 kg-robot LWRIII, the 54 kg-robot KR3-SI, the 235 kg-robot KR6, and the 2350 kg-robot KR500. The HIC is rated according to the EuroNCAP Assessment Protocol And Biomechanical Limits. All produced HIC values at impact velocities up to 2 m/s range in the green area. This indicates that only very low head injury occurs during the impacts. Furthermore, the previously described saturation effect of the HIC can be observed. The HIC is displayed for impact test with a Hybrid III-dummy (denoted by HIII) and with a simplifying setup (denoted by DD) mimicking the behavior of the Hybrid III-dummy head.

The Head Injury Criterion (HIC) was the first automobile injury indicator introduced into the robotics literature [2], [3]. As extrapolated from robot-dummy impacts with the DLR Lightweight Robot (LWRIII) in [4] a saturation of the Head Injury Criterion at a certain impact velocity with increasing robot mass is observed. In [5] this effect was confirmed with heavy-duty industrial robots and a simplified test-setup mimicking the characteristics of a Hybrid III-dummy (HIII) head. In Fig. 1 the HIC values for all tests presented in [4], [5] and the ones shown in *Part I* are depicted up to an impact velocity of 2 m/s and classified according to the EuroNCAP [6]. First, it is clearly confirmed that our HIII-head imitating device reproduces similar HIC values to the HIII. Furthermore, the mentioned saturation effect is confirmed by the fact that the KR6 and the KR500 produce very similar HIC values for equivalent impact speed by means of standardized crash-test measurements. In general, the obtained HIC values for speeds up to 2 m/s are classified

as subcritical. By means of the EuroNCAP only *very low* injury can occur. Although this clearly confirms that the human head is not in a critical situation at velocities up to 2 m/s, the question arises whether other body parts, such as the neck, would be posed to a serious threat during the post-impact phase of such a collision. This questions aims to an answer whether the neck stiffness and body inertia are constructed such that the neck is the weak point or not, leading us to the next case: The description of the head-neck-torso complex dynamics during a rigid blunt impact.

B. Case 2: Timing Properties of the Head-Neck-Torso Complex During Fast Head Impacts

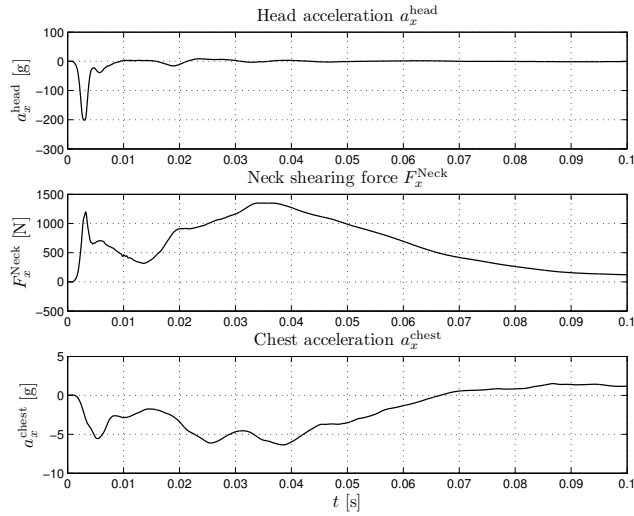


Fig. 2. The dynamics behind a frontal head impact with the KR500.

In the robotics literature the head impact and the corresponding HIC evaluation was usually treated as an isolated event between the robot and the human head. The head was generally assumed to act decoupled from the torso during the short acceleration pulse that defines the impact dynamics. In the present case we discuss this assumption on an experimental basis.

In Fig. 2 the time courses of the head acceleration, the neck force, and the acceleration of the chest in x -direction are depicted for a head collision at an impact velocity of 4.1 m/s with the KR500. The head acceleration peak occurs timely along with a peak in the neck force (the load cell is mounted between head and neck which is a quite stiff construction). Delayed to that, the torso starts accelerating and reaches its maximum value several milliseconds after the head acceleration and neck force passed their peak values. The impact phase is followed by a continuous bending of the neck and a longer acceleration phase of the torso. One can see in x -direction the decoupling assumption really holds to a certain extent. However, it has to be mentioned that the z -acceleration (not displayed here) of the chest was observed to lag only 1 ms behind the maximum impact acceleration. This seems to be an effect caused by the very high neck stiffness of the HIII compared to a human. Due to this tight

neck coupling a clear separation of head and torso during the initial impact does not occur in z -direction.

In contrast to this observation [7] states that the human head is indeed decoupled during an impact at 3.2 ms from T1¹. Furthermore, [8] points out that the neck of the HIII is only to a certain extent able to predict human neck injury due to its much higher stiffness properties. In order to get more realistic dynamics it seems to be desirable to use a dummy which spine has more biofidelity than the one of the HIII, e.g. the BIO-RID-II.

After discussing the timing properties of a head impact and the related neck force and chest acceleration, the connected question whether significant neck injury occurs during such a robot-head impact is treated in the following.

C. Case 3: Neck Injury During Head Impacts

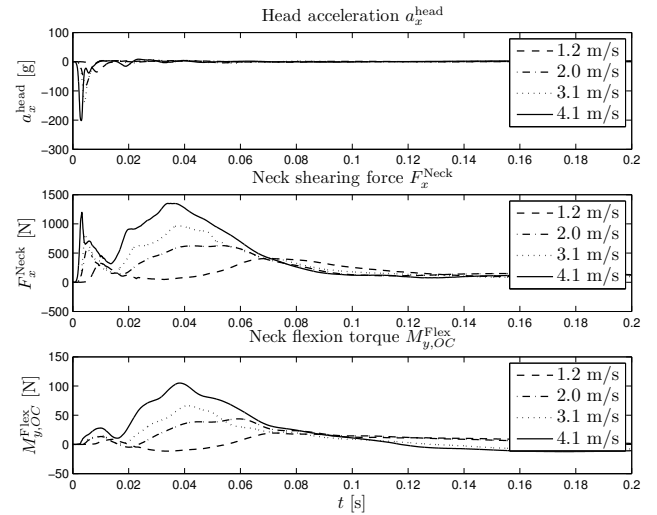


Fig. 3. The head acceleration a_x^{head} and neck force F_x^{Neck} in x -direction as well as the neck flexion moment during a frontal head impact with the KR500 at increasing robot speed. The robot behaves due to its large inertia as a velocity source and drags the head further away while the neck is bended and the trunk accelerates due to the transmitted force.

In the present case we discuss the question whether the head can be accelerated during an impact powerful enough such that the trunk cannot follow before the neck forces and torques exceed their corresponding tolerance thresholds. The question we want to answer is: Is it possible that, although HIC is small during an unconstrained impact, the human suffers severe neck injury? With our previous dummy tests in [4] we were not able to analyze this because at high velocities the maximum joint torques of the LWRIII are exceeded. This causes the brakes of the robot to engage in order to protect it. Thus, the robot is not able to further drag the head and potentially injure the neck any more. During the short duration of the initial impact the neck is definitely not posed to critical loads with impact speeds up to 2 m/s. Since the motion of the 2350 kg-robot KR500 is not affected by

¹The human spine can be divided into the cervical, thoracic, and lumbar spine. T1 is the first thoracic vertebra.

the collision with the dummy² due to its large inertia it can be treated as a velocity source during an impact and is suited to evaluate this question.

In Fig. 3 the head acceleration, the neck force in x -direction, and the torque about the occipital condyles are depicted for impact velocities up to 4.1 m/s with the KR500. The head acceleration is caused by the short impact which defines the Head Injury Criterion and the maximum head acceleration. The neck force shows a similar peak in the beginning, followed by a second wider one. Please note that the first and second maximum are more or less equally large. For the neck torque the first maximum shows only marginal growth with increasing impact velocity while the second peak value increases with impact velocity. The second maximum is in both cases caused by the continuous motion of the robot which further bends the neck while the trunk begins to accelerate.

In general, neck forces tend to be more dangerous the longer they are applied to the neck. Therefore, it is easily evident that a heavy robot, not affected in its motion during the impact, increases the injury potential significantly. As shown in *Part I* the neck forces reach *very high* injury levels only at maximum velocity³ (above 4 m/s) by means of the EuroNCAP. In case of the neck flexion torques following observations can be made. Although they increase significantly with impact velocity, no more than to 100 Nm, which is still under the limit value, are reached. In the limited extend in which a HIII is able to predict neck injury, one is able to conclude that only very high impact velocities could pose a threat to the neck during head impact. Up to 2 m/s which we believe to be a desirable (high) speed in physical-human robot interaction no significant injury level can be observed by means of the evaluated criteria.

One can therefore conclude that the frontal unconstrained blunt head impact poses no threat below 2 m/s both, in terms of HIC and indirect effects on the neck. A look at frontal unconstrained chest collisions and their characteristics shall now be taken.

D. Case 4: Chest Injury

In the robotics literature [2], [3], [4] it was usually emphasized that the human head has to be treated very carefully in a safety analysis due to its fragility. This is of course the most intuitive approach and is certainly a reasonable choice. In this sense the outcome of the tests we will discuss now is somewhat surprising at a first glance since it shows that the

²Please not that even for the 235 kg-robot KR6 the current monitoring was triggered at high speeds, i.e. also for this robot the maximum joint torques are exceeded. Furthermore, the robot loses significantly momentum during the impact due to its lower inertia compared to the KR500.

³In order to evaluate the injury severity correlating to the measured neck forces on a worst-case basis with respect to the corresponding EuroNCAP rating we chose to determine the real maximum exceedance interval as an upper bound estimate. Instead of determining the maximum exceedance time we use the smallest rectangle that fits for the particular index and use its width as the exceedance time and the height as the corresponding value of the injury index. This leads to an upper bound and therefore to a more restrictive evaluation of neck forces.

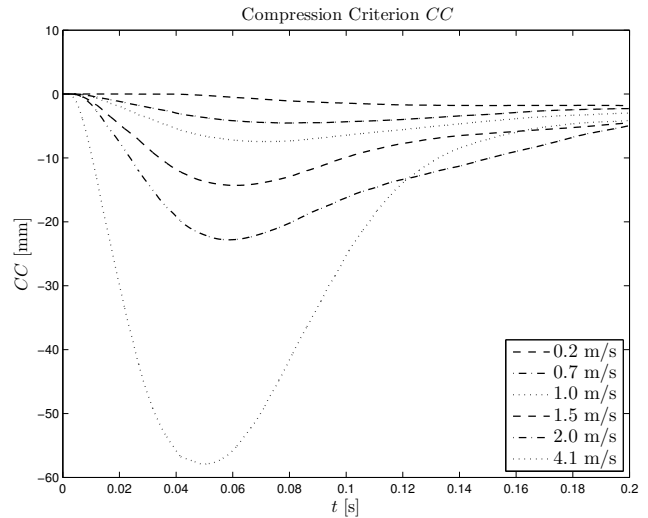


Fig. 4. Compression Criterion for chest impact up to 4.1 m/s with the KR500.

chest is posed to at least the same threat as the head and is unambiguously reaching critical injury levels.

Fig. 4 depicts the time courses of the Compression Criterion (CC) during frontal chest impacts with the KR500 at impact velocities up to 4.1 m/s. The impact duration of more than 150 ms is significantly larger compared to the 5 ms for the head impacts. The corresponding main reasons for this fact are the large inertia of the dummy body and the lower stiffness of the chest compared to the one of the head. In *Part I* it was shown that except for the maximum resulting head acceleration, all head criteria during head impacts are in the *very low* injury severity region for an impact velocity of up to 3.2 m/s. Only for the KR6 at maximum velocity of 4.2 m/s an HIC value slightly above the threshold from *very low* to *low* was observed. While facing *low* injury for the head impacts (when not considering the pure maximum acceleration) an aspect that seems for us quite surprising is that, according to the chest impact results, the CC indicates *very high* injury severity at maximum velocity for the KR6 and the KR500, c.f. Fig. 4. Apparently, the inertia of the dummy trunk delays the motion such that the robot compresses the chest up to potentially lethal dimensions even in the unconstrained case. Furthermore, already at 2.0 m/s the threshold from *very low* to *low* injury is crossed for the KR500, showing that the injury potential starts to become dangerous.

For the unconstrained impact, one can therefore conclude (while excluding the maximum resulting head acceleration from the analysis) that the chest impact is surprisingly the most critical one for heavy robots. We analyze now the influence of an increasing barrier, i.e. the role of partial constraints.

E. Case 5: The Partially Constrained Impact

Fig. 5 shows the neck compression force for partially constrained head impacts with varying barrier height h_B (for details on the setup please refer to *Part I*). The neck

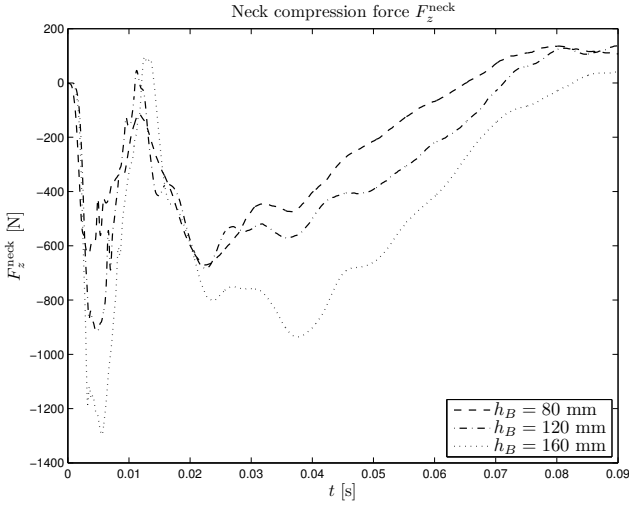


Fig. 5. Compression Criterion for chest impact up to 4.1 m/s with the KR500.

force F_z increases significantly with increasing h_B up to a neck force of -1296 N with $h_B = 160$ mm compared to -670 N with $h_B = 80$ mm. The second peak also shows dependency on the barrier height. Unfortunately, we cannot confirm this statement as clearly for the neck shearing force and torque. Furthermore, the generally lower impact criteria compared to the unconstrained head impacts (see *Part I* for the exact numerical values) are presumably caused by a slightly different location of the dummy during the partially constrained impacts. Nonetheless, although at the current state we are not able to explicitly determine the lethal threshold height, it is intuitively clear that such a height must exist. Further tests are therefore necessary to analyze this effect more in detail and be able to predict the threshold height for a barrier. Furthermore, it is crucial to take a closer look at eventual spine injury during partially constrained impacts. Because the HIII is not able to measure this effect this is left for future research with distinguished equipment.

Another interesting observation made during the partially constrained impact is that a second impact occurs with the barrier obstructing the motion of the trunk. This is not the case for the non-constrained case in which the dummy moves away fast enough to avoid a second impact with the robot.

F. Case 6: The Constraint Quasistatic Impact with the LWRIII

As shown in [9] any robot is theoretically able to exceed the fracture tolerance of the facial and cranial bones in case the human head is clamped and the robot drives through a singularity (see *Part I* and [9] for the full problem description). A prerequisite for this to happen is for a particular bone with tolerance force $F_{\text{frac}}^{\text{bone}}$ and stiffness K_{bone} that the distance to singularity has to be

$$d_s \geq \frac{F_{\text{frac}}^{\text{bone}}}{K_{\text{bone}}}.$$

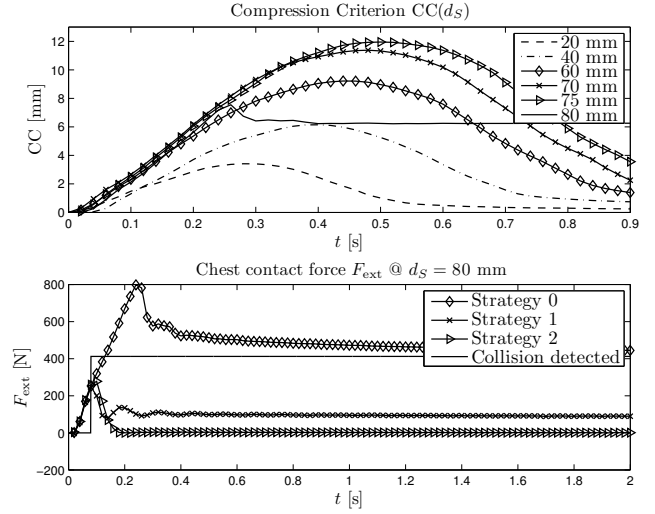


Fig. 6. Singularity clamping with the LWRIII and a HIII. The measured CC is displayed for different values of d_S (upper). The chest contact force for $d_S = 80$ mm is depicted for the base case and two collision strategies (lower).

Although this is theoretically possible it is still the question whether in reality a particular robot would be able to withstand such large forces or whether unmodeled structural compliances prevent the occurrence of this worst-case. In *Part I* we show various constrained head and chest impacts with the LWRIII driving through the singularity in outstretched configuration and leading to the observation that the tolerance values of both, head and chest are not exceeded.

In Fig. 6 (upper), the CC is plotted for varying values of the distance to singularity d_s . There are two factors affecting the maximally reachable force, depending on the contact point d_s :

- 1) If the contact point is too close to the singularity (d_s is small), then the maximal force is limited by the compliance of the chest, which deflects and allows the robot to pass through the singularity.
- 2) If the contact point is far from the singularity ($d_s > 80$ mm), then the contact force is limited by the maximal joint torques, since the Jacobian is not ill-conditioned any more. A low level safety stop is activated when maximal joint torques are exceeded, preventing the further increase of the force.

Under these circumstances, the maximal compression, namely 11.95 mm, was reached for $d_s = 75$ mm. Although an exceedance of the threshold values is not possible for this impact type, please keep in mind that the achievable CC value is, compared to the unconstrained dynamic impacts presented in [4], more than twice as high.

Apart from the discussed worst-case behavior, the effect our collision detection and reaction [10] has on such an impact shall now be explained. In Fig. 6 (lower) the resulting force profiles are plotted and the collision detection signal indicated. Clearly, the potential threat is cleared quickly after the collision is detected. For every impact configuration the

detection is sensitive enough to detect the collision. Both reaction strategies are leading to a significant contact force reduction.

This constrained quasistatic impact can be used as both, a worst-case analysis concerning maximum contact force and as a benchmark problem for a collision detection and reaction scheme which is only based on proprioceptive sensing as the one treated in the present case.

Up to now we discussed various cases which treat different aspects relevant for future robotics safety standards defined for physical Human-Robot Interaction. In the next section we give a proposal of impact tests which are from our perspective absolutely necessary for a full safety evaluation of robotic systems.

III. STANDARD IMPACTS

In this section we will give, based on our results with robot-dummy crash-testing, some recommendations with respect to a more standardized view on this topic. If future robotic systems are going to act around humans and cooperate with them by physical means, a standardized crash-testing protocol will be needed to evaluate different robots on a meaningful and comparable basis. In this sense we want to initiate this process by proposing *Standard Impact Phases* for the unconstrained impact, leading to a set of *Standard Impact Tests* for analyzing robot-human safety.

A. Standard Impact Phases

In order to define standard impact tests one has to take into consideration the complexity of a collision process. It does not only consist of the immediate instance of interaction lasting only a few milliseconds but a much more intricate process is directly related to it. This incorporates the behavior of the human body and its physical interaction with the robot and the environment. Establishing safety during head collisions is not only about determining the apparent head injury but it has to take into consideration all phases of a collision and the injury potential related to them. The following definition of major phases for the free unconstrained impact shows that already this simplest case of a robot-human collision is consisting of (minimally) five major phases, as can be extracted from the high-speed videos.

- **Phase I:** The short phase in which the direct impact between robot and head takes place.
- **Phase II:** The neck starts moving significantly due to the motion of the head.
- **Phase III:** The trunk begins to move significantly.
- **Phase IV:** The head loses contact with the robot and the entire body moves freely in space.
- **Phase V:** The body impinges on the ground usually first with the trunk and then with the head: The secondary impact occurs.

A pictogram visualizing these phases is shown in Fig. 7. Analogue to the head impact it is quite straight forward to define similar phases for the chest. These standard phases are a good starting point to formulate standard impacts for robotics. A proposal that seems from our current state

of knowledge a reasonable suggestion is outlined in the following.

B. Standard Dummy Impact Tests

The following impact test proposal is from our point of view as a suitable starting point for a standardized set of blunt impacts tests. In this proposal we exclude the evaluation of upper and lower extremities due to the fact that except for first experiments presented in [11] this is still a very open issue in robotics.

A) Sitting configuration

I – Frontal impact

- Impact regions
 - Head
 - Chest
- Varying Barrier height $0 \dots h_B^{T1}$

II – Side impact

- Impact regions
 - Head
 - Chest
 - Abdomen
 - Pelvis
- Varying Barrier height $0 \dots h_B^{T1}$

III – Rear impact

- Impact regions
 - Head
 - Chest
- Varying Barrier height $0 \dots h_B^{T1}$

B) Standing configuration

I – Frontal impact

- Impact regions
 - Head
 - Chest
 - Abdomen
 - Pelvis
- Varying Barrier height $0 \dots h_B^{Leg}$

II – Side impact

- Impact regions
 - Head
 - Chest
- Varying Barrier height $0 \dots h_B^{Leg}$

III – Rear impact

- Impact regions
 - Head
 - Chest
- Varying Barrier height $0 \dots h_B^{Leg}$

In order to consider the complexity of robot-human impacts we first suggest to distinguish between a collision between a robot and A) a sitting dummy and B) a standing dummy. Furthermore, the major impact directions for collisions have to be covered, leading to the necessity of frontal, side, and rear impacts for which distinguished crash-test dummies exist. Then, the different impact locations are

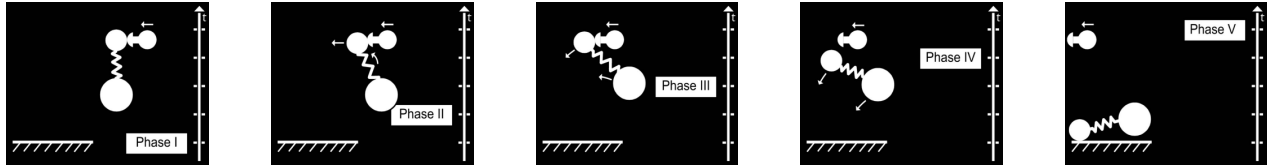


Fig. 7. Standard impact phases for an unconstrained robot-head impact. This can be applied to any single contact impact model, consisting of two bodies connected via a junction.

chosen according to the sensorial equipment of the particular dummy. Please note that the impact to the head should be directed normally towards the center of gravity of the head (partially adjustable with the head tilting angle φ_N) and the impacts at the other body parts have to act directly on the particular sensor. Additionally to simply hitting the dummy in free space, varying barriers are proposed to evaluate the effect of constraints in the environment. For sitting configuration they should maximally range to the trunk height of the dummy h_B^{T1} (T1 denotes the first thoracic vertebra) and for the standing configuration up to the leg height h_B^{Leg} of the dummy. The heights h_I^H , h_I^C , h_S , h_B , h_I^P , and h_I^A have to be selected according to the specific dummy suited for the impact type. The aim of these tests is to provide a set of well defined testing setups which allow not only to evaluate the direct impacts (Phase I) but also the subsequent motion (Phase II-IV) and even the secondary impact (Phase V). All following tests assume a hard basement on which the secondary impact occurs. Therefore, the question about the consequences after the collision phase can be answered as well. In principle arbitrary further situations can be imagined but we believe that this set of impact tests provides, similarly to automobile crash-testing, a clear evaluation of injury severity for blunt impacts. From high-speed recordings it becomes clear which part of the recorded signals correlates to the particular impact phase and thus a separate analysis of each phase is possible. The main reason to distinguish between sitting and standing condition is, apart from the influence of partial constraints, a more detailed analysis of related secondary impacts. These will mainly depend on impact velocity and drop height.

The motion of the robot is commanded such that it moves at a constant velocity and all impacts tests are to be carried out up to maximum velocity of the robot under the impact direction constraint. To quantify the effects of collision detection and reaction schemes for a robot it is important to show under which conditions they contribute to increasing safety and where their limitations are located. The analysis we presented for the LWRIII can be seen as a first template.

It is very clear that performing the entire set of measurements is an expensive and time consuming issue. However, the tests are related to different injury types, which do not obviously correlate. Therefore, we believe that they are mandatory in an incipient phase. Of course, if it turns out that a subset of the tests captures all relevant aspects, a reduction

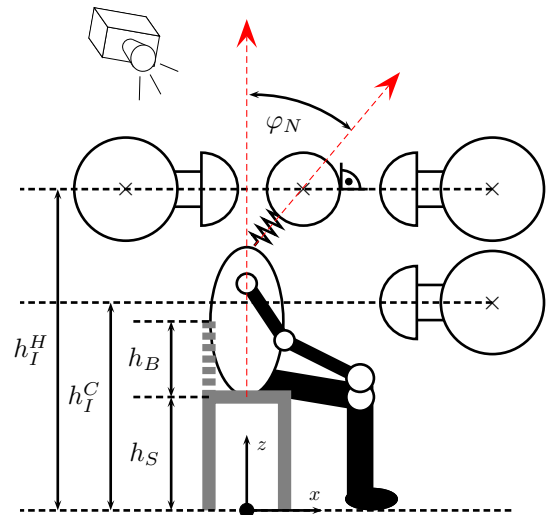


Fig. 8. Standard frontal sitting head and chest impact test and standard sitting rear impact.

of the test extent will be done.

1) *The Standard Sitting Frontal and Rear Impact:* In Fig. 8 the *frontal sitting* and *rear sitting* setup are shown. The dummy is sitting upright on a fixed object at height h_S and the head is adjusted such that the dummy is hit in normal direction against the head. The impact locations in this setup are the head and chest in the frontal case and the head only for rear impacts. The head is hit at h_I^H and the chest at h_I^C . In order to evaluate partial constraints the barrier height h_B is elevated until no further increase of injury severity is observed or the dummy is in danger to be destroyed.

2) *The Standard Sitting Side Impact:* In Fig. 9 the *side sitting* setup is depicted. The dummy is sitting upright on a fixed object at height h_S and $\varphi_N = 0^\circ$ (The head is oriented horizontally such that the robot hits the dummy normal to the occiput.). The impact locations tested in this setup are the head, the chest, the abdomen, and the pelvis. The head is hit at h_I^H , the chest at h_I^C , the abdomen at h_I^A , and the pelvis at h_I^P . In order to evaluate partial constraints the side barrier height h_B is elevated until no further increase of injury severity is observed or the dummy could be destroyed.

3) *The Standard Standing Frontal and Rear Impact:* In Fig. 10 the *frontal standing* and *rear standing* setup are shown. The dummy is standing upright and the head is

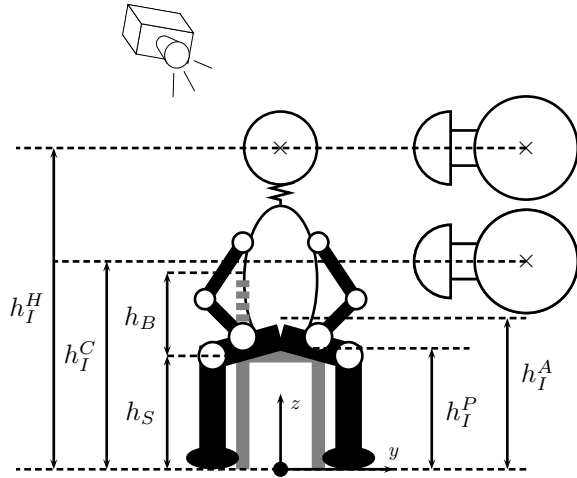


Fig. 9. Standard sitting side head, chest, and abdomen impact test.

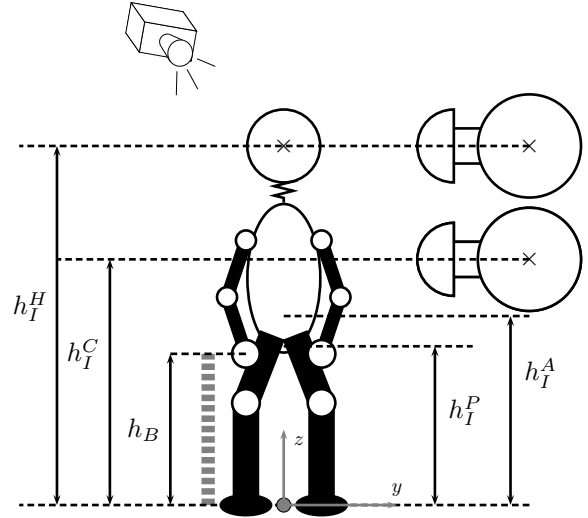


Fig. 11. Standard standing side head, chest, and abdomen impact test.

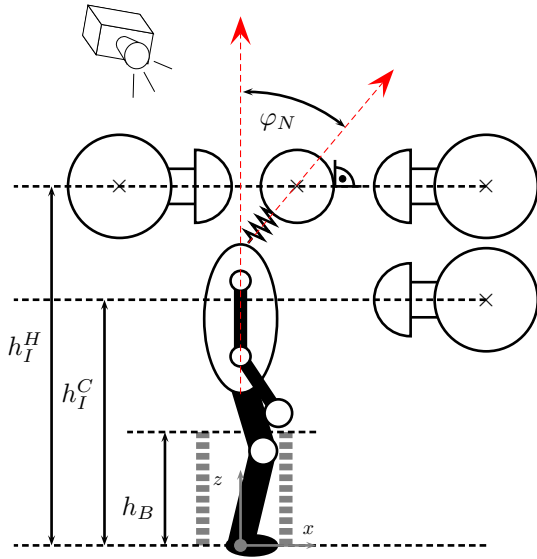


Fig. 10. Standard frontal standing head and chest impact test and standard standing rear impact.

adjusted such that dummy is hit in normal direction against the head. The impact locations tested in this setup are the head and chest in the frontal case and the head for rear impacts. The head is hit at h_I^H and the chest at h_I^C . In order to evaluate partial constraints the barrier height h_B (in the back of the dummy for frontal impacts and in front of the dummy for rear impacts) is elevated until no further increase of injury severity is observed or the dummy could be destroyed.

4) *The Standard Standing Side Impact:* In Fig. 11 the *side standing* setup is depicted. The dummy is standing upright. The impact locations tested in this setup are the head, the chest, the abdomen, and the pelvis. The head is hit at h_I^H , the chest at h_I^C , the abdomen at h_I^A , and the pelvis at h_I^P . In order to evaluate partial constraints the side barrier height h_B is elevated until no further increase of injury severity is

observed or the dummy could be destroyed. Please note that in this test the barrier does only affect the lower extremities.

In order to carry out all these experiments, various testing devices become necessary. Therefore, we will now give a list of crash-test devices that are suitable in this sense.

C. Crash-test Dummies for Robot-Human Impacts

Impact test	Proposed dummy
Sitting frontal	Hybrid III 50th Percentile Male
Sitting side	EuroSID-1/EuroSID-2 (ES-2)
Sitting rear	BioRID-II
Standing front	Pedestrian or Hybrid III with standing support
Standing side	EuroSID-1/EuroSID-2 (ES-2) with standing support
Standing rear	BioRID-II with standing support

TABLE I

DUMMIES FOR STANDARDIZED CRASH-TESTING IN ROBOTICS.

In Table I appropriate crash-test dummies for each of the proposed standard tests by biomechanical dimensioning are listed. They provide rich sensorial equipment and are tailored to the needs of the proposed impact tests. The first two for *Sitting frontal* and *Sitting side* are already established dummies in automobile crash-testing. The BioRID-II was designed for the rear impact assessment and is among other things especially designed for whiplash assessment. The Pedestrian can be used to simulate secondary impacts and their dependency on impact velocity and robot mass. As an alternative one could fix a Hybrid III in standing position and realize a simple release mechanism e.g. based on a light barrier to simulate standing during the impact.

IV. OUTLOOK

In future work we would like to extend our proposal to following body parts for the three impact directions.

- Frontal impact
 - Knee, femur, pelvis
 - Lower leg
 - Upper Extremities
 - Cranium: mandible, maxilla, nasal,...
- Side impact
 - Cranium: temporal, parietal
- Rear impact
 - Spine
 - Cranium: parietal, occipital

For these listed body parts distinguished dummies exist which will be used for detailed analysis in the future. The standardized evaluation of the face could be analyzed with face dummies as presented in [12], [13] and even further aspects as the eye with the new FOCUS (facial and ocular countermeasure for safety headform), developed by Denton [14]. Of course, some of these tests are only worth to be carried out for pHRI-robots and not for large industrial robots. Apart from defining standardized blunt impact testing, it is absolutely necessary to get to a point at which soft-tissue injury can be evaluated in a standardized way as well. First evaluations in this direction were carried out in [15].

V. CONCLUSION

Current standardization efforts as ISO-10218 seem from our perspective too preliminary and they are hardly capturing real-world requirements. Since a differentiated analysis of injury mechanisms and the understanding of major factors behind them are missing, the recommendations for realizing safety are very restrictive limits for the robot performance. However, if future systems are supposed to collaborate with humans and achieve high performance, a detailed and comparative analysis of robotics systems is necessary in order to get the maximum performance at an acceptable risk of injury under certain worst-case conditions. Consequently, in this work we provide experimental background on which future standards could base on. Furthermore, we give a proposal on how future standardized blunt crash-testing could be formulated. The definition of such regulations makes it possible to compare different robots objectively and assess their qualification for human-robot interaction.

ACKNOWLEDGMENT

This work has been partially funded by the European Commission's Sixth Framework Programme as part of the project PHRIENDS under grant no. 045359. We would like to thank the ADAC and especially Daniel Schindler for their excellent collaboration and for contributing such valuable expertise. Furthermore, we would like to thank KUKA Roboter GmbH for their financial support and especially Dr. Tim Guhl for his help with the experiments. Further thanks go to Michael Strohmayer for his greatly acknowledged help.

REFERENCES

- [1] ISO10218, "Robots for industrial environments - Safety requirements - Part 1: Robot," 2006.
- [2] A. Bicchi and G. Tonietti, "Fast and Soft Arm Tactics: Dealing with the Safety-Performance Trade-Off in Robot Arms Design and Control," *IEEE Robotics & Automation Mag.*, vol. 11, pp. 22–33, 2004.
- [3] M. Zinn, O. Khatib, and B. Roth, "A New Actuation Approach for Human Friendly Robot Design," *Int. J. of Robotics Research*, vol. 23, pp. 379–398, 2004.
- [4] S. Haddadin, A. Albu-Schäffer, and G. Hirzinger, "Safety Evaluation of Physical Human-Robot Interaction via Crash-Testing," *Robotics: Science and Systems Conference (RSS2007)*, 2007.
- [5] —, "The Role of the Robot Mass and Velocity in Physical Human-Robot Interaction - Part I: Unconstrained Blunt Impacts," in *IEEE Int. Conf. on Robotics and Automation (ICRA2008)*, Pasadena, USA, 2008, pp. 1331–1338.
- [6] EuroNCAP, "European Protocol New Assessment Programme - Frontal Impact Testing Protocol," 2004.
- [7] R. Nightingale, J. McElhaney, D. Camacho, M. Kleinberger, B. Winkelstein, and B. Myers, "The Dynamic Responses of the Cervical Spine: Buckling, End Conditions, and Tolerance in Compressive Impacts," *Proceedings of the 41st Stapp Car Crash Conference*, vol. SAE Paper No.973344, pp. pp. 771–796, 1997.
- [8] B. Herbst, S. Forrest, D. Chng, and A. Sances, "Fidelity of Anthropometric Test Dummy Necks in Rollover Accidents," *Proceedings of the 16th ESV Conference*, vol. Paper No. 98-S9-W-20, 1998.
- [9] S. Haddadin, A. Albu-Schäffer, and G. Hirzinger, "Safe Physical Human-Robot Interaction: Measurements, Analysis & New Insights," in *International Symposium on Robotics Research (ISRR2007)*, Hiroshima, Japan, 2007.
- [10] A. De Luca, A. Albu-Schäffer, S. Haddadin, and G. Hirzinger, "Collision Detection and Safe Reaction with the DLR-III Lightweight Manipulator Arm," *IEEE/RSJ Int. Conf. on Intelligent Robots and Systems (IROS2006)*, pp. 1623–1630, 2006.
- [11] S. Haddadin, A. Albu-Schäffer, A. De Luca, and G. Hirzinger, "Collision Detection & Reaction: A Contribution to Safe Physical Human-Robot Interaction," in *IEEE/RSJ Int. Conf. on Intelligent Robots and Systems (IROS2008)*, Nice, France, 2008.
- [12] D. Viano, C. Bir, T. Walilko, and D. Sherman, "Ballistic Impact to the Forehead, Zygoma, and Mandible: Comparison of Human and Frangible Dummy Face Biomechanics," *The Journal of Trauma*, vol. 56, no. 6, pp. 1305–1311, 2004.
- [13] J. Melvin, W. Little, J. Smrcka, Z. Yonghau, and M. Salloum, "A Biomechanical Face for the Hybrid III Dummy," *Proceedings of the 39th Stapp Car Crash Conference*, 1995.
- [14] "www.dentonatd.com."
- [15] S. Haddadin, A. Albu-Schäffer, A. De Luca, and G. Hirzinger, "Evaluation of Collision Detection and Reaction for a Human-Friendly Robot on Biological Tissue," in *IARP International Workshop on Technical challenges and for dependable robots in Human environments (IARP2008)*, Pasadena, USA. [Online]. Available: <http://www.robotic.de/Sami.Haddadin>